Photodiagnosis and Photodynamic Therapy 25 (2019) 227–236

Contents lists available at ScienceDirect

Photodiagnosis and Photodynamic Therapy

journal homepage: www.elsevier.com/locate/pdpdt

Photoactivated resveratrol against *Staphylococcus aureus* infection in mice

Denisar Palmito dos Santos, Diego Patrick Soares Lopes, Ricardo Costa de Moraes Junior, Caroline Vieira Gonçalves, Luciano Pereira Rosa, Francine Cristina da Silva Rosa, Robson Amaro Augusto da Silva*

Federal University of Bahia, Anísio Teixeira Campus- Multidisciplinary Institute in Health, 58 Rio de Contas Street – 17 Block – 58 Lot, Candeias, ZIP 45.029-094, Vitória da Conquista, Bahia, Brazil

A R T I C L E I N F O

Keywords:
Staphylococcus aureus
Photodynamic therapy
Resveratrol

A B S T R A C T

Background: Among the pathogens, *Staphylococcus aureus* is the main causative agent of bacterial diseases in the world. In this context, antimicrobial photodynamic therapy (aPDT) appears as a promising tool by means of microbial inactivation with the use of light. aPDT is applied in treatments involving photosensitizers capable of generating oxygen free radicals. Thus, this work proposes the use of resveratrol as a photosensitizer.
Methods: *In vitro* tests were performed to determine the antibacterial activity of photoactivated resveratrol with blue LED light, as well as uric acid experiments for verification of singlet oxygen formation. Possible resveratrol structural changes were evaluated by HPLC. In the *in vivo* assays, the air pouch model was performed in mice for antimicrobial activity and cytokine production.
Results: The photoactivated resveratrol exhibited an increase in its antibacterial action and it is possibly brought about by the singlet oxygen formation. In the air pouch model, TNF-α and IL-17A cytokines were produced, diminishing the bacterial load, and consequently, reducing inflammation after 24 h of infection. Cellular number decrease in the inflammatory environment was associated with resolution of inflammation along with greater IL-10 production.
Conclusion: It is the first time that resveratrol has been associated with aPDT. It was demonstrated in this work that resveratrol activated by blue LED light can be a promising photosensitizer. This compound, after the light stimulus, produces singlet oxygen, in addition to having effects on the immune system triggering TNF-α and IL-17A production, aiding in the clearance of several bacteria, including *S. aureus*.

1. Introduction

Bacterial infections occur worldwide and constitute a major public health problem [1]. With the introduction of antimicrobials, the survival of infected people has increased, however, over the years, some strains have become resistant to traditional compounds used in the therapeutic practice [2,3].

Among the pathogens, *Staphylococcus aureus* is the main causative agent of bacterial diseases. Infections by this microorganism have led to the death of millions of people annually, especially due to its advanced mechanisms of virulence [4]. Isolates of this infectious agent that are resistant to methicillin are called MRSA (Methicillin-resistant *Staphylococcus aureus)* [5]. Therefore, outbreaks of community-based infections by resistant strains present a wide distribution in the terrestrial environment resulting in increase in the necessity for developing new strategies to prevent and treat such disorders.

Most *S. aureus* strains are now resistant to penicillin, MRSAs are common in hospitals and are emerging in the community. Penicillinase-resistant penicillins (flucloxacillin, dicloxacillin) remain the antibiotics of choice for the management of serious methicillin-susceptible *S. aureus* (MSSA) infections. First generation cephalosporins (cefazolin, cephalothin and cephalexin), clindamycin, lincomycin, and erythromycin have important therapeutic roles in mild MSSA infections such as in skin and soft tissue, or in patients with penicillin hypersensitivity, although cephalosporins are contraindicated in patients with immediate penicillin hypersensitivity (urticaria, angioedema, bronchospasm or anaphylaxis) [5,6].

Therefore, new antimicrobial therapies are critical. In this context, antimicrobial photodynamic therapy (aPDT) follows similar principles to the photodynamic therapy (PDT) ones, which is more widely known for its application in non-cancerous diseases and cancerous lesions therapeutic [7]. This technique is used in treatments involving

* Corresponding author.
E-mail address: robson.amaro@gmail.com (R.A.A. da Silva).

https://doi.org/10.1016/j.pdpdt.2019.01.005
Received 10 July 2018; Received in revised form 22 November 2018; Accepted 4 January 2019
Available online 07 January 2019

photosensitizers capable of generating oxygen free radicals when activated at a given wavelength by light emitted through a laser [8,9].

It has already been shown that aPDT is capable of inactivating MRSA strains through two distinct photodynamic processes [10,11]. Upon light activation, an excited photosensitizer can undergo type I (electron transfer) and/or type II (energy transfer) reactions to produce highly reactive oxygen species (ROS). Type I reactions generate radical anion species, while type II reactions produce singlet oxygen [12–14].

Hence, the research on new photosensitizers development becomes important, especially for providing alternative therapeutic resources for the persistent infections healing process. In addition, there is no report of resistance to the aPDT, and the financial investment required for the new photosensitizer studies is lower when compared to a traditional antimicrobial drug [15].

Thus, this work presents the use of photoactivated resveratrol by light. This polyphenol, especially present in grape, promotes health benefits through its anti-angiogenic, anti-inflammatory and antimicrobial activity [16–21]. In the initial studies, it was characterized as a phytoalexin. Since then, several studies have begun to point out its correlation with the prevention or reduction of tumor progression, cardiovascular clinical conditions, among others. Recent works have shown that this polyphenol is capable of interacting with light sources, even changing its structure [22,23].

Faced with the promising ability of resveratrol, several studies correlated this compound and the immune system. In many of them, it was observed its interaction with cells and inflammatory response factors, mainly by regulating the proinflammatory cytokines production [24–26]. There are no reports on the resveratrol use in photodynamic therapy in the treatment of bacterial infections, being this a pilot study.

In this context, this work aimed to evaluate the use of photoactivated resveratrol by blue LED light in the treatment of *S. aureus* in an air pouch model of infection in mice.

2. Materials and methods

2.1. MRSA strains

The MRSA ATCC 43300 strain was obtained from the Federal University of Bahia –Multidisciplinary Institute in Health - Anísio Teixeira *Campus*. The samples were stored in a freezer at −80 °C (Equilam, São Paulo, Brazil). At the time of culture, they were thawed at room temperature, plated on Brain Heart Infusion agar (BHI, pH7.4, HIMEDIA), and taken to the incubator (Prolab, São Paulo, Brazil) for 24 h at 37 °C.

2.2. Determination of bacterial inoculum

The determination of the bacterial load was executed by spectrophotometry. It was performed by means of the direct suspension, and carried out in previously sterilized laminar flow (Prolab, São Paulo, Brazil), through the removal of 3 to 5 colonies from the culture plates and their dilution in 1 mL of sterile saline. Subsequently, an aliquot of this solution was placed in quartz cuvettes for reading on the spectrophotometer (Prolab, São Paulo, Brazil).

At this time, the following parameters have to be reached: 0.135 absorbance at 660 nm (0.5 in the McFarland scale, equivalent to 1.5×10^8 CFU/mL), in order to obtain 10^8 CFU of MRSA. The suspension was seeded on the surface of the Brain Heart Infusion agar (BHI, pH 7.4, HIMEDIA).

2.3. Resveratrol photoactivation

The resveratrol (PharmaNostra, Campinas, São Paulo) was obtained from the Federal University of Bahia – Multidisciplinary Institute in Health – Anísio Teixeira *Campus*. For *in vitro* and *in vivo* antimicrobial activity assays, the compound was solubilized in propylene glycol in a sterile environment, and used at a concentration of 2 mg/mL.

The resveratrol photoactivation was performed through the incident light by a prototype device number 1.012960-3 (MM Optics, São Carlos, São Paulo, Brazil) that have five blue LEDs with a wavelength of 450 ± 20 nm. Irradiation procedure was carried out for 5 min, power density of 75 mW/cm^2, for a total fluence delivered of 54 J/cm^2.

2.4. In vitro antimicrobial activity evaluation

The *in vitro* antimicrobial evaluation test was carried out following the literature, with adaptations [27]. In a 24-well plate, 10^8 CFU of MRSA were added in 1 mL of BHI broth (BHI, pH 7.4, HIMEDIA) in each well. Subsequently, the formation of groups were performed: six wells were left in the dark and received no treatment (Group 1 – MRSA), six wells were treated with only blue LED light (Group 2 – MRSA + Blue LED light), six wells received twenty microlitres of resveratrol and were kept in the dark (Group 3 – MRSA + resveratrol), finally, six wells received twenty microlitres of resveratrol and blue LED light (Group 4 – MRSA + photoactivated resveratrol). The concentration of resveratrol and the photoactivation protocol were the same as described above.

After the execution period of the photoactivation protocol, five microliters from each well were seeded on a BHI medium plate. The tests were performed in triplicate and the CFU counts were performed after the time of 6, 12, 18 and 24 h. Free open source software, ImageJ (NIH), was used to count CFUs.

2.5. Analysis by UV–vis spectroscopy

For the spectrophotometric and high performance liquid chromatography (HPLC) techniques, a mass of 100 mg of resveratrol, after dissolution in an aqueous ethanol solution (Merckmillipore, Darmstadt, Germany), was transferred to a volumetric flask of 1000 mL. Then, the volume of the flask was filled with the aqueous ethanol solution (95%) until a stock solution containing resveratrol at a concentration of 100 mg/L. Afterwards, 1 mL of this solution was transferred to a 100 mL volumetric flask. The volume of the flask was quenched with ethanol until an intermediate solution containing resveratrol at the concentration of 0,001 mg/mL.

Uric acid was used to verify if resveratrol photoactivation produces reactive oxygen species. In order to reach that, the solutions were analyzed before and after the photoactivation. The light activation protocol was the same as described above. Therefore, the resveratrol solution described and a solution of 30 μg/mL of uric acid (Bioclin, São Paulo, Brazil) were analyzed by spectrophotometry (UV-1800 - Shimadzu Scientific Instruments), at room temperature. This spectrophotometer operates in the Spectral range of 200–900 nm. Quartz cuvettes (Analiticaweb, São Paulo, Brazil) with Optic path of 1.0 cm and capacity of 4 mL were used. The same resveratrol solution was used in the (HPLC) technique.

2.6. HPLC instrumentation and conditions

The HPLC system consisted of a Gynkotek M 580 GT pump, Rheodyne 8125 injector (20-μL loop) (Cotati, CA), and a Gynkotek M 340S UV diode-array detector (Gynkotek GmbH, Germering, Germany). A column (250 × 4.6 mm) packed with 6 μm particle size C18 material was used for the separations. Chromeleon data management software (Dionex Corp., Sunnyvale, CA) was used for equipment control and for data evaluation.

A multistep gradient method was applied using methanol–water–acetic acid (10:90:1, v/v) mixture as solvent A and methanol–water–acetic acid (90:10:1, v/v) mixture as solvent B at a flow rate of 1.5 cm^3/min (the reagents supplier was Quimisul, Santa Catarina, Brazil). The gradient profile was: 0.0–18.0 min, from 0% to 40% B; 18.1–25.0 min, from 40% to 100% B; and 25.1–27.0 min, 100% B. Chromatographic separations were monitored at 306 nm. Chromatographic peaks were identified by comparing the samples retention time with the ones belonging to the standard compounds in the literature.

2.7. Animals

C57BL/6 mice aging from six to eight weeks were obtained from the UFBA-IMS/CAT facilities. The animals were maintained under controlled conditions of temperature with free access to water and food. The animal challenge was performed using the air pouch model. All procedures involving animals were approved by the Ethics Committee on Animal Use (CEUA) IMS-CAT UFBA, under protocol number 042/2017.

2.8. The air pouch model

The manufacture of the air pouch was carried out as described in the literature, with variations [28–30]. Initially, the animals were anesthetized with 50 mg/kg of ketamine (Vetnil, São Paulo, Brasil) and 10 mg/kg of xylazine (Vetnil, São Paulo, Brasil). In each mouse 3 mL of sterile air was inoculated into the dorsal subcutaneous space. Mice challenged with MRSA received 10^7 CFU of inoculum resuspended in 100 µL of saline.

In the *in vivo* experiments, resveratrol was solubilized in sterile propylene glycol (Quimisul, Santa Catarina, Brazil). Thus, groups of animals challenged with sterile propylene glycol (**Control, group 1**), animals challenged with 10^7 CFU of MRSA (***MRSA*, group 2**), animals challenged with 10^7 CFU of MRSA and 100 µL of Resveratrol (2 mg/mL) (***MRSA* + Resveratrol, group 3**), and finally, animals challenged with 10^7 CFU of MRSA and 100 µL of photoactivated Resveratrol (2 mg/mL) (**MRSA + Photoactivated Resveratrol, group 4)** were set up. After photoactivation, resveratrol was immediately inoculated into the air pouch in the treated animals. The concentration and volume were the same as that in the *in vitro* assay.

Then, 24 h post infection, the animals were euthanized (n = 6/group). The euthanasia of the animals was performed by deep anesthesia with intraperitoneal administration of ketamine and xylazine at doses of 400 mg/kg and 40 mg/kg, respectively.

2.9. Inflammatory cell influx

The lavages of air pouch were performed with 5 mL of sterile saline and stored at 4 °C. Later, the fluid was centrifuged at the conditions of 300 g for 10 min at 4 °C. The total cell count was done in a Neubauer chamber (Prolab, São Paulo, Brazil). The differential cell counts were performed by cytocentrifuge (Cytopro®) in Panoptic stained slides and analyzed by light microscopy (Olympus, Münster, NRW, Germany). The remaining fluid was stored at −80 °C for later quantification of cytokines by Enzyme-Linked Immunosorbent Assay (ELISA).

2.10. Bacterial load

Five microliters of lavages were seeded on BHI plates and incubated at 37 °C for 24 h. The technique used was the pour plate, thus facilitating the quantitation of the number of colonies formed after culture time [30]. The CFU quantification was performed with the aid of a colony counter (CP-600 Plus, Phoenix), at 12 and 24 h.

2.11. Quantification of inflammatory cytokines in the air pouch lavages

The supernatant extracted from the air pouch lavages were used to quantify TNF-α, IL-1β, IL-10 or IL-17A cytokines by sandwich ELISA using the ELISA Ready-SET-GO® kit (*Bioscience*), according to the manufacturer. A standard curve was obtained, and the cytokines in the samples were calculated according to the manufacturer´s instructions.

2.12. Histological study

Samples of the air pouch skin were collected, fixed in 10% formalin, and embedded in paraffin. These samples were sectioned at 5 µm, and stained by Hematoxilin and Eosin (Laborclin, Pinhais, Brazil). Histological slides of each animal were analyzed through light microscopy using an optical microscope Olympus® (Olympus, Münster, NRW, Germany) coupled to a camera Olympus SC30 (Olympus, Münster, NRW, Germany) for pathological alterations evaluation. Pictures from each animal sample were taken using analysis getIT® (version 5.2, Olympus Soft Imaging Solutions, Münster, NRW, Rhine-Westphali, Germany).

2.13. Statistical analysis

Statistical analyses of the experiments were performed using the *Kruskal-Wallis* test through GraphPad Prism® software (version 5.0, GraphPad Program Inc., San Diego, CA, USA), and Dunn´s as post-test. For other outcomes, we used the *Mann-Whitney* test to make comparisons between groups. Statistical differences were considered significant at p value < 0.05.

3. Results

3.1. Photoactivated resveratrol promotes increase in the inhibition of bacterial growth in vitro

The Fig. 1 demonstrates that there was greater inhibition of bacterial growth in the culture plates treated with the photoactivated form of Resveratrol.

3.2. Resveratrol has photodynamic activity generating singlet oxygen

To analyze the mechanism of antimicrobial action of the compound formed after resveratrol stimulation with blue led light, an uric acid

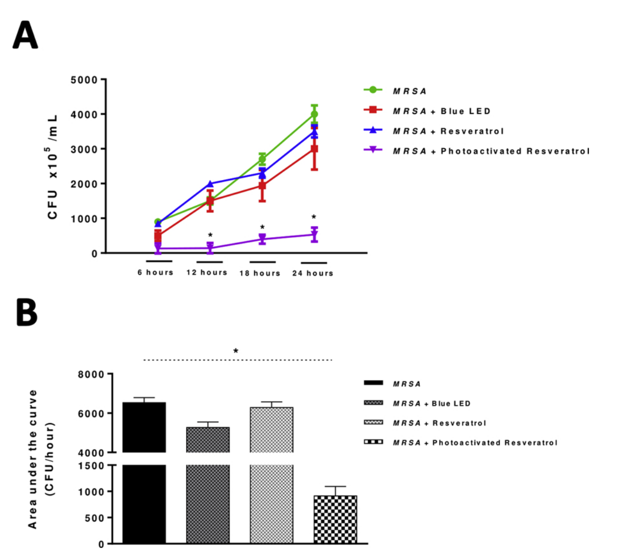

Fig. 1. Bacterial Load of *Staphylococcus aureus* (CFUx10^5 /mL) - In a 24-well plate, 10^8 CFU of MRSA were added in 1 mL of BHI broth. Subsequently, six wells were left in the dark and received no treatment (Group 1 - MRSA), six wells were treated with only blue LED light (Group 2 - MRSA + Blue LED light), six wells received twenty microlitres of resveratrol and were kept in the dark (Group 3 MRSA + resveratrol), finally, six wells received twenty microlitres of resveratrol and blue LED light (Group 4 – MRSA + photoactivated resveratrol). After the period of execution of the photoactivation protocol, five microliters from each well were seeded on a BHI medium plate and the counts of the CFUs were performed after the time of 6, 12, 18 and 24 h (A) and the area under the curve was measured (B). (* p < 0.05).

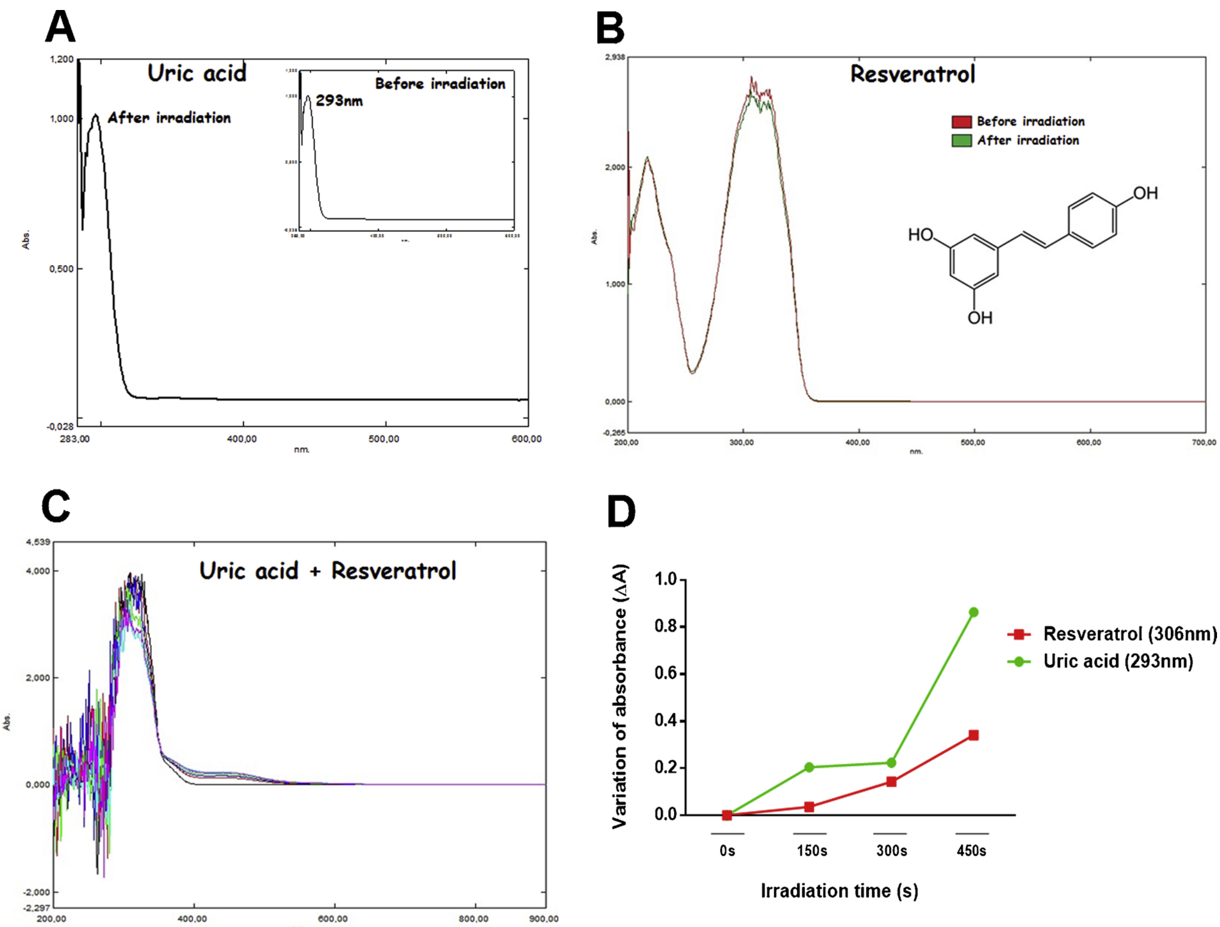

Fig. 2. UV/Visible Spectroscopy analysis of a resveratrol and uric acid solution – The solutions of 0001 mg/mL resveratrol and 30 µg/mL uric acid were prepared for analysis. Uric acid did not change absorbance after being submitted to the photoactivation protocol (A). The resveratrol used in this experiment showed its characteristic absorbance at 306 nm (B). After mixing the solutions of resveratrol and uric acid followed by the photoactivation protocol, the reduction in the absorbance of the solution as a function of time (C) was observed. In view of this, the variation of the absorbances of the two solutions as a function of time (D) was calculated.

solution was photoactivated along with the resveratrol solution described above. The uric acid absorbance variation was observed as a function of the irradiation time due to a uric acid photo-oxidation *via* singlet oxygen produced by photoactivated resveratrol (after photoactivation).

3.3. Photoactivated resveratrol exhibits change in retention time in HPLC analysis

To analyze whether the photoactivation causes some type of alteration in resveratrol, HPLC (Fig. 3) analysis was performed. The tests were conducted for both the photoactivated and no photoactivated form.

3.4. Therapy using photoactivated resveratrol as a photosensitizer reduces the number of inflammatory cells in the air pouch

To assess whether there were quantitative differences in inflammatory cells in the air pouch, the inflammatory environment lavage was analyzed for total and differential count of inflammatory cells. As seen in Fig. 4, data obtained demonstrate that there was a reduction in total inflammatory cells in the animals treated with the photoactivated resveratrol. There was also a reduction in the number of cells in the air pouch skin, as it can be seen in the images analysis.

3.5. Photoactivated resveratrol enhances the release of TNF-α and IL-17 into the air pouch

With the objective of analyzing animals treated with photoactivated resveratrol, a production profile on differentiated IL-1β, IL-10, TNF-α, and IL-17A cytokines was conducted. The air pouch lavages were analyzed by ELISA. Animals treated with the photoactivated compound presented greater TNF-α and IL-17A production (Fig. 5).

3.6. Animals treated with photoactivated resveratrol demonstrated greater levels of bacterial clearance in the air pouch

The Fig. 6 presents the bacterial growth behavior after 24 h of cultivation. It was observed that C57Bl/6 mice treated with photoactivated resveratrol had lower formation of CFU than the non-treated group.

4. Discussion

S. aureus infections constitute a public health problem due to the large numbers of resistance cases of this pathogen to the traditional antimicrobials, additional to the fact the medicines production is a rather slow process, and consequently, the development of new active compounds does not follow such growth. This work brings a new proposal for the treatment of these infections by using resveratrol activated with blue light as an alternative.

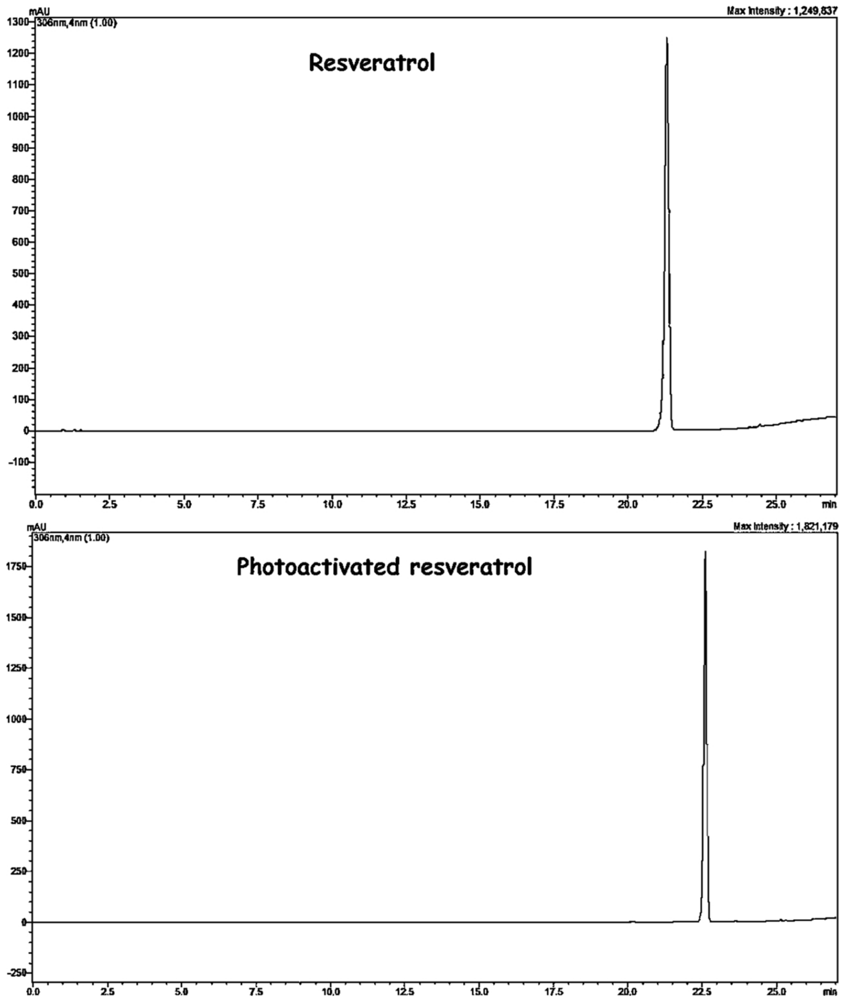

Fig. 3. HPLC chromatograms of Resveratrol - A 0.001 mg/mL resveratrol solution was prepared for analysis. Analyses of photoactivated and no photoactivated compounds were performed. Chromatographic separations were monitored at 306 nm.

It was observed that this association was able to reduce bacterial growth, both *in vitro* and *in vivo*, showing lower local inflammation and higher levels of cytokines production, such as TNF-α and IL-17, besides the generation of singlet oxygen. In addition, it is possible that the light irradiation had caused structural changes in the resveratrol molecule, since the compound presented a change in its retention time in the HPLC analysis after the photoactivation. In that way, it is likely the resveratrol absorbs photons and undergoes photochemical, and chemical reactions that lead it to become a biologically active compound with bacteriostatic activity.

The current literature conveys works presenting the resveratrol photostimulation under several different light sources. When exposed to the sunlight, this compound undergoes a molecular rearrangement whose structure consists of two fused aromatic rings attached to a linear chain containing a carbonyl group conjugated to a double bond, in which the authors termed the molecule obtained as "Resveratrone" [22,23]. With LED light, authors have reported the glycosylation of resveratrol. The use of blue LEDs as light source for the resveratrol biotransformation has remarkably improved the yield of its β-D-glycosides and changed the composition of products, the 3-O-β-D-glucoside was the major product. [31].

Once it is a pilot study, it is not possible to say that resveratrone or 3-O-β-D-glucoside was formed in our experiment, however, it can be affirmed that resveratrol had the ability to interact with blue LED light, modifying its structure (Fig. 3), and exhibiting antimicrobial action (Figs. 1 and 6).

The uric acid is an efficient singlet oxygen sensor acting as a chemical dosimeter for the quantitative determination of the photodynamic action of a compound [32,33]. The Fig. 2 shows its optical absorption spectrum and photo-oxidation. Initially, the light stimulation of uric acid was performed in the wavelength range studied for this study. Therefore, as noted in Fig. 2A, the wavelength range used herein was not able to change the absorbance of the compound, which ensures that the interaction with the light is restricted to the resveratrol in the experiments of determination of photodynamic activity.

Fig. 2D shows the absorbance variation of the uric acid bands (293 nm) and resveratrol (306 nm) as a function of the irradiation time. The photo-oxidation reaction of uric acid *via* singlet oxygen is well-known, and lead to the formation of products such as triurea, alantoxaidin, oxanate ion and CO_2, occurring the suppression of singlet oxygen by uric acid with the capture of the triplet state energy of the resveratrol molecule in the excited state by the uric acid molecule. Further, this highly reactive oxygen athom initiates oxidative reactions in the proximate environment, like the bacterial cell wall, lipid membranes, enzymes, or nucleic acids [34].

When we associate resveratrol with uric acid with subsequent photoactivation we noticed a reduction in the absorbance profiles of the two molecules (Fig. 2D). The literature classifies this effect as photobleaching, being a characteristic directly related to the therapeutic dose of the compound with photodynamic activity [35]. Accordingly, here it was presented a decay of the characteristic band signal of uric acid at 293 nm, indicating that the decomposition reaction of this molecule

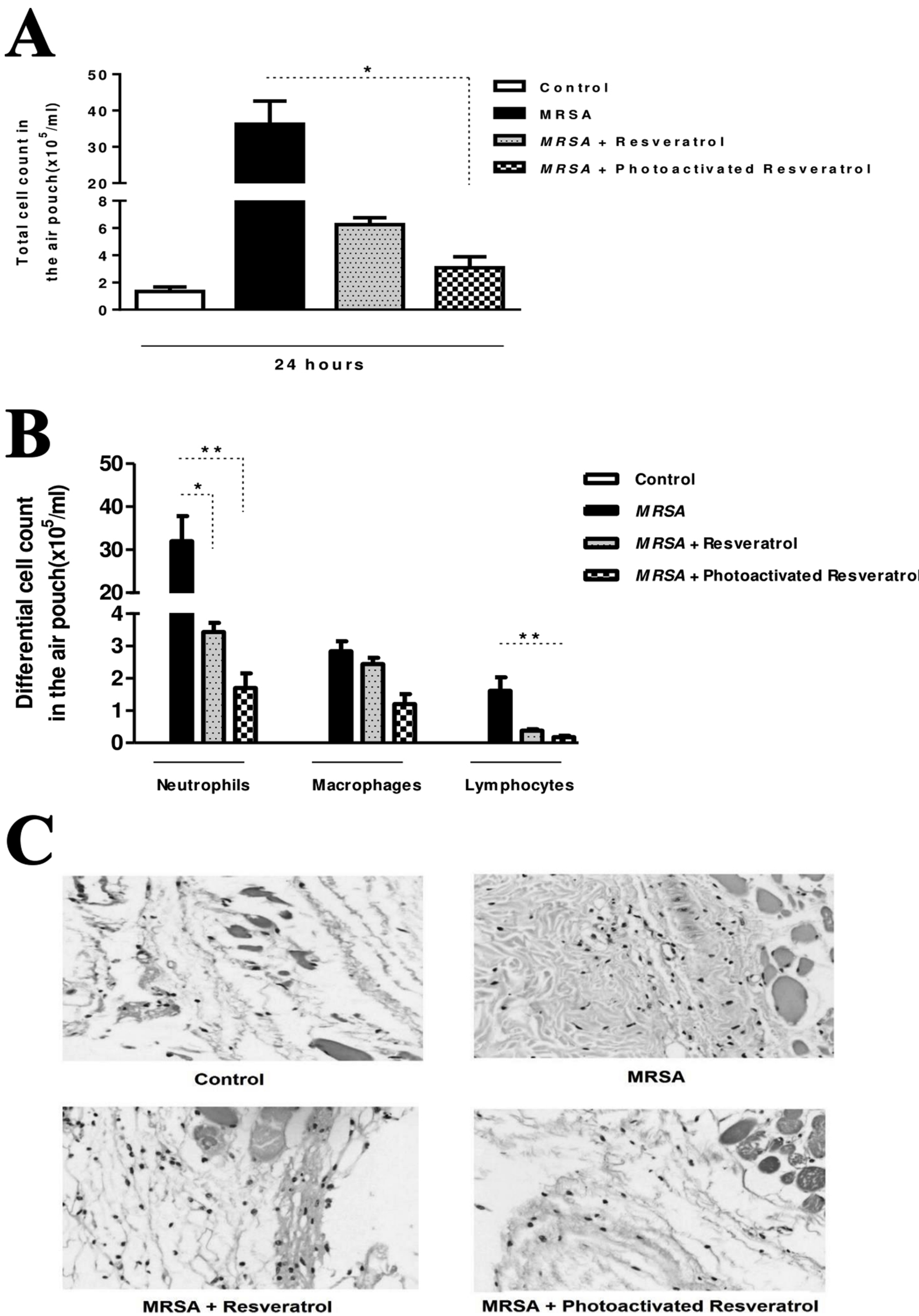

Fig. 4. Total and differential counts of leukocytes in the air pouch lavages and visualization of inflammation in the air pouch skin (x10^5/mL) - Skin samples from the air pouch were removed (collected), fixed in 10% formalin, and stained by hematoxilin and eosin. After slides production, the total (A) and differential (B) counts of the leukocytes were performed, as well as the representative images of the histological slides (C). (n = 6); (BHI = brain heart infusion; MRSA: Methicillin-resistant *Staphylococcus aureus*); (* $p < 0.05$, ** $p < 0.01$).

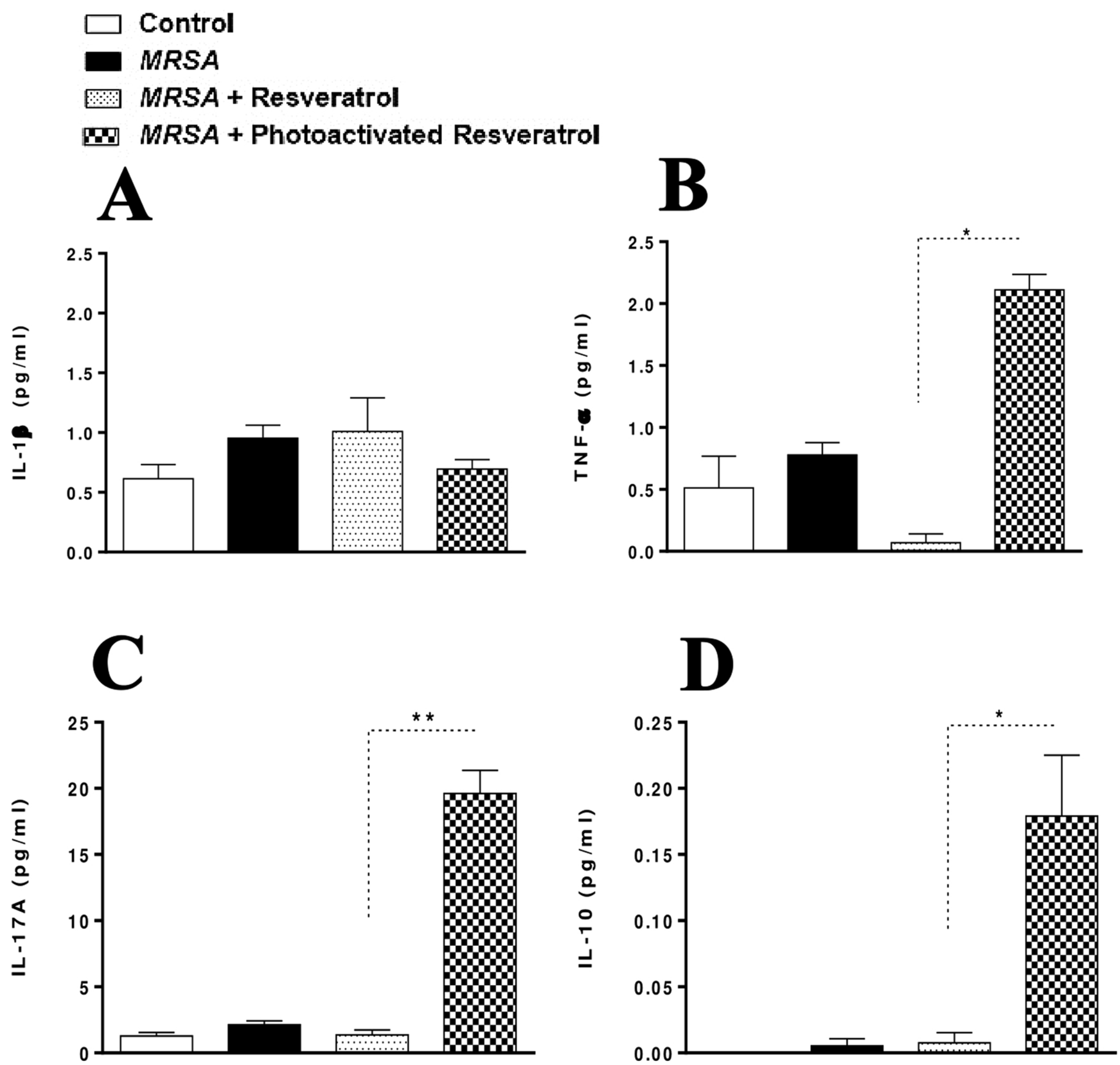

Fig. 5. Quantification of cytokines in the inflammatory environment (pg/mL) - Lavages from air pouch were collected later and evaluated by ELISA for the presence of IL-17A, IL-10, IL-1β and TNF-α. (n = 6); (BHI = brain heart infusion; MRSA: Methicillin-resistant *Staphylococcus aureus*);(* $p < 0.05$, ** $p < 0.01$).

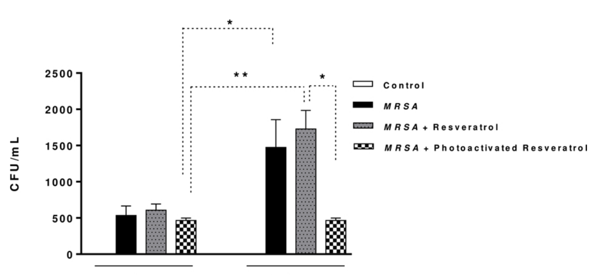

Fig. 6. Bacterial Load of *Staphylococcus aureus* in the air pouch (CFUx10^5/mL) – Lavages from air pouch were collected later and cultured in BHI. The CFUs were quantified after 24 h. (n = 6); (BHI = brain heart infusion; MRSA: Methicillin-resistant *Staphylococcus aureus*);(* $p < 0.05$, ** $p < 0.01$).

occurs through the singlet oxygen formed by the excited resveratrol.

These results support raising the theory on that the photostimulated resveratrol antimicrobial action is by the generation of reactive oxygen species. The products generated from the reactions are cytotoxic, but singlet oxygen has been considered the main responsible for the antimicrobial effect of aPDT. The antimicrobial effect of the photosensitizer can happen by producing sufficient quantity of singlet oxygen nearby the outer membrane of the bacteria, so that it can diffuse into the cellular interior, culminating in lethal damage. As a consequence, the photosensitizer must be in close contact with the target cell in such a way the singlet oxygen generated can exert its antimicrobial effect, since it presents a small diffusion distance (20 nm) and short half-life time [36–38].

The great difficulty in developing an effective treatment against *S. aureus* is for the reason this pathogen is part of the human microbiota, and is in understanding which type of inflammatory response is effective in the clearance of this microorganism. Several studies in the attempt to develop immunoprotection have failed to develop a prophylactic method against infections by this pathogen [39–41]. Thus, works that seek complementary forms of traditional antimicrobial therapies present promising results. PDT has been used to combat staphylococcal infections for a long time [42–45]. Many of these works use curcumin as a photosensitizing agent [11,46].

However, even if there are few reports of resistance to aPDT, it is possible that the development of resistant strains occur. Since it is a new therapy, with expansion in its use it cannot be assured that resistance will not come out [47]. aPDT has short half-life time and acts based on the attack of multiple cellular targets by photo-generated ROS; then, a prior concept is that the development of resistance to the aPDT is unlikely [48]. However, there are reports in literature indicating that some *S. aureus* strains are more tolerant to the aPDT than others, and the findings that some clinical isolates demonstrated decreased susceptibility of to the aPDT after photodynamic exposure, point out a need for detailed investigations on bacterial adaptive responses to photodynamic treatment [48–51].

Therefore, it is necessary to increase the photosensitizers availability, as it is necessary to develop new antimicrobials. To date, studies have sought to determine adequate parameters for clinical application of aPDT, which involves assessing different photosensitizers, light sources and doses, and drug concentrations [52,53]. On that account, researches have aimed to identify photosensitizers with antimicrobial activity when associated with LED light, a lower cost light source and simpler technology in comparison to the laser devices, facilitating the clinical application of this therapy [54].

In addition, when compared to other antimicrobial therapies, aPDT has many advantages such as higher specificity (the photosensitizer can be delivered to the cell and can be highly focused to the site of injury in cases of cutaneous treatment), and fewer undesirable side effects [55,56]. Given these facts, we chose to use Resveratrol activated by blue light because of its antimicrobial activity, additionally to its structural similarity as other photosensitizers as phenolic groups, like the curcumin.

Moreover, the resveratrol in the UV/Visible spectrum sweep presents an absorption band at 306 nm. Then, the light emission is close to the maximum absorption range of the molecule. However, this is not a rule, since there are studies that stimulate photosensitizers in several bands of wavelength and not only in the maximum absorption range [57–61]. In this work, we photoactivated propylene glycol, and found that this compound did not exhibit inhibition of bacterial growth *in vitro*. Taking this into consideration, we used propylene glycol as a solvent for resveratrol in the experiments.

The photoactivation of the solutions were performed outside the body environment of the C57Bl/6 animals, since the melanin could be an interfering agent in the aPDT [51]. Therefore, here we are proposing an adaptation of aPDT for the treatment of infections in black patients, since in the literature, there are few studies evaluating this technique in these patients [62]. After photoactivation, the solutions were immediately applied to the animals. The air pouch model is a convenient *in vivo* model to study localized inflammation without systemic effects [63]. In this context, it was possible to observe the effects of photoactivated resveratrol against a MRSA infection in a live model.

What can be inferred from the results obtained through this study is that the interaction of photoactivated resveratrol with the immune system becomes evident (Fig. 4). Notably the stimulation of the release of important cytokines such as TNF-α and IL-17 (Fig. 5). This is fundamental for the clearance of *S. aureus*, which have already been reported in several works [64,65]. The stimulation of their release is a determining factor for the treatment, especially in infections by resistant strains.

It has been shown that knockout mice for IL-17 are unable to effectively eliminate *S. aureus*. In that way, immune responses associated with Th17 cells could be a strategic target to eradicate persistent infections in humans [66]. Many studies have described that this cytokine is produced by T lymphocytes, but most of this component in inflammatory processes is secreted by cells of the innate immunity [67]. The release of IL-17A by neutrophils has been described by different authors [68,69]. Mice deficient in IL-17A or IL-17F have proved prone to skin infections caused by gram-positive bacteria such as *S. aureus* [70]. Experimental models using immunogens associated with a Th17 response against pathogens such as *S. aureus* and *Candida albicans* demonstrated an increase in recruitment and activation of phagocytes at infection sites, in addition to the more effective clearance of these pathogens in tissues [71]. In this context, the IL-17 production in the induction of effector mechanisms against *S. aureus* and the presence of cells that produce this cytokine is fundamental for the infection control.

Increased release of TNF-α is an interesting finding, since there are conflicting data in literature on the Resveratrol ability to alter the production of this cytokine. We found that in the our group where this polyphenol was not photoactivated, actually occurred a reduction in the release of TNF-α. Different studies have shown the importance of the TNF-α release, a pro-inflammatory cytokine, with the reduction of MRSA infection associated with laser therapy [72–75]. Furthermore, aPDT stimulates macrophages to release TNF-α in great quantities, leading to an increase of this cytokine at the site of inflammation [76–79]. The leukocytes activated by TNF-α produce reactive species of oxygen and nitrogen, essential for the elimination of microorganisms. In that way, the immune system cells activation by TNF-α is essential for the infections control [80,81].

Quantitatively, the number of inflammatory cells in the resveratrol-treated groups was lower than in non-treated ones (Fig. 4A). This data corroborates with several works showing that after the treatment of animal models with this polyphenol, there was a local inflammation reduction [82]. However, in our data, even with a reduction in the number of cells in the site, the inhibition of bacterial growth was greater (Fig. 6), a fact, since the exacerbation of the local inflammation can be harmful to the organism. Moreover, it is possible that even in a smaller quantity, the inflammatory cells are directed by the synergism of IL-17A and TNF-α [83,84], resulting in a greater) reduction of the bacterial load, even with a lower cell number.

On the other hand, it is possible that 24 h after treatment with photoactivated resveratrol, time analyzed by our work, the decrease in number of inflammatory cells has already occurred due to the bacterial clearance. This fact would also explain the higher levels of IL-10 production (Fig. 5D), an anti-inflammatory cytokine, secreted to modulate inflammatory responses [85]. No differences were observed between the groups regarding IL-1β production. In addition to these data, the air pouch model was one of the factors that aided in the effective visualization of inflammation, since it is easy to manipulate and obtain clinical samples that help in the understanding of the local inflammatory response.

Considering the results obtained in this work, we can see that resveratrol activated by blue LED light can be a promising photosensitizer to be used in antimicrobial photodynamic therapy. This compound, after the light stimulus, produces singlet oxygen, a potent antimicrobial, combined to the fact it was able to exert effects on the immune system with TNF-α and IL-17A production, which are pro-inflammatory cytokines, aiding in the clearance of several bacteria, including *S. aureus*. Since it is a pioneering work, more studies are necessary to allow a clear elucidation of the mechanism of action of photoactivated resveratrol.

Disclosure of conflict of interests

The authors have no conflicts of interests to declare.

Funding

This study was funded by the Institutional Program of Scientific Initiation of Federal University of Bahia for the Scientific Initiation scholarships awarded, and by the Research Center in Optics and Photonics (CePOF) for the equipment to the development of this work. Authors want to acknowledge financial support from CAPES (Coordenação de Aperfeiçoamento de Pessoal de Nível Superior) foundation for the phD grant.

References

[1] C. Alvarez, J. Labarca, M. Salles, Prevention strategies for methicillin-resistant *S taphylococcus aureus* (MRSA) in Latin America, Braz. J. Infect. Dis. 14 (Suppl 2) (2010) S107–118.

[2] R.P. Wenzel, M.B. Edmond, Vancomycin-resistant *Staphylococcus aureus*: infection control considerations, Clin. Infect. Dis. 27 (1998) 245–249 quiz 250-241.

[3] A.R. Gomes, H. Westh, H. de Lencastre, Origins and evolution of methicillin-resistant *Staphylococcus aureus* clonal lineages, Antimicrob. Agents Chemother. 50 (2006) 3237–3244.

[4] G.Y. Liu, Molecular pathogenesis of *Staphylococcus aureus* infection, Pediatr. Res. 65 (2009) 71R–77R.

[5] F.D. Lowy, *Staphylococcus aureus* infections, N. Engl. J. Med. 339 (1998) 520–532.
[6] L.C. Gelatti, R.R. Bonamigo, A.P. Becker, P.A. d Azevedo, Methicillin-resistant *Staphylococcus aureus*: emerging community dissemination, An. Bras. Dermatol. 84 (2009) 501–506.
[7] A. Hanakova, K. Bogdanova, K. Tomankova, K. Pizova, J. Malohlava, S. Binder, R. Bajgar, K. Langova, M. Kolar, J. Mosinger, H. Kolarova, The application of antimicrobial photodynamic therapy on *S. aureus* and *E. coli* using porphyrin photosensitizers bound to cyclodextrin, Microbiol. Res. 169 (2014) 163–170.
[8] M.M. Gois, C. Kurachi, E.J. Santana, E.G. Mima, D.M. Spolidorio, J.E. Pelino, V. Salvador Bagnato, Susceptibility of *Staphylococcus aureus* to porphyrin-mediated photodynamic antimicrobial chemotherapy: an *in vitro* study, Lasers Med. Sci. 25 (2010) 391–395.
[9] F. Vatansever, W.C. de Melo, P. Avci, D. Vecchio, M. Sadasivam, A. Gupta, R. Chandran, M. Karimi, N.A. Parizotto, R. Yin, G.P. Tegos, M.R. Hamblin, Antimicrobial strategies centered around reactive oxygen species–bactericidal antibiotics, photodynamic therapy, and beyond, FEMS Microbiol. Rev. 37 (2013) 955–989.
[10] Y. Guo, S. Rogelj, P. Zhang, Rose Bengal-decorated silica nanoparticles as photosensitizers for inactivation of gram-positive bacteria, Nanotechnology 21 (2010) 065102.
[11] P.P. Almeida, I.S. Pereira, K.B. Rodrigues, L.S. Leal, A.S. Marques, L.P. Rosa, F.C. da Silva, R.A.A. da Silva, Photodynamic therapy controls of *Staphylococcus aureus* intradermal infection in mice, Lasers Med. Sci. 32 (2017) 1337–1342.
[12] L. Huang, Y. Xuan, Y. Koide, T. Zhiyentayev, M. Tanaka, M.R. Hamblin, Type I and Type II mechanisms of antimicrobial photodynamic therapy: an *in vitro* study on gram-negative and gram-positive bacteria, Lasers Surg. Med. 44 (2012) 490–499.
[13] L.M. de Freitas, E.N. Lorenzon, N.A. Santos-Filho, L.H.P. Zago, M.P. Uliana, K.T. de Oliveira, E.M. Cilli, C.R. Fontana, Antimicrobial photodynamic therapy enhanced by the peptide aurein 1.2, Sci. Rep. 8 (2018) 4212.
[14] H. Ding, H. Yu, Y. Dong, R. Tian, G. Huang, D.A. Boothman, B.D. Sumer, J. Gao, Photoactivation switch from type II to type I reactions by electron-rich micelles for improved photodynamic therapy of cancer cells under hypoxia, J. Control. Release 156 (2011) 276–280.
[15] H. Abrahamse, M.R. Hamblin, New photosensitizers for photodynamic therapy, Biochem. J. 473 (2016) 347–364.
[16] D. de Sa Coutinho, M.T. Pacheco, R.L. Frozza, A. Bernardi, Anti-inflammatory effects of resveratrol: mechanistic insights, Int. J. Mol. Sci. 19 (2018).
[17] Z.X. Zhou, S.F. Mou, X.Q. Chen, L.L. Gong, W.S. Ge, Anti-inflammatory activity of resveratrol prevents inflammation by inhibiting NFkappaB in animal models of acute pharyngitis, Mol. Med. Rep. 17 (2018) 1269–1274.
[18] A. Lancon, R. Frazzi, N. Latruffe, Anti-oxidant, anti-inflammatory and anti-angiogenic properties of resveratrol in ocular diseases, Molecules 21 (2016) 304.
[19] N. Bostanghadiri, A. Pormohammad, A.S. Chirani, R. Pouriran, S. Erfanimanesh, A. Hashemi, Comprehensive review on the antimicrobial potency of the plant polyphenol Resveratrol, Biomed. Pharmacother. 95 (2017) 1588–1595.
[20] M. Chalal, A. Klinguer, A. Echairi, P. Meunier, D. Vervandier-Fasseur, M. Adrian, Antimicrobial activity of resveratrol analogues, Molecules 19 (2014) 7679–7688.
[21] M.M. Chan, Antimicrobial effect of resveratrol on dermatophytes and bacterial pathogens of the skin, Biochem. Pharmacol. 63 (2002) 99–104.
[22] I. Yang, E. Kim, J. Kang, H. Han, S. Sul, S.B. Park, S.K. Kim, Photochemical generation of a new, highly fluorescent compound from non-fluorescent resveratrol, Chem. Commun. (Camb.) 48 (2012) 3839–3841.
[23] T. Rodriguez-Cabo, I. Rodriguez, M. Ramil, R. Cela, Comprehensive evaluation of the photo-transformation routes of trans-resveratrol, J. Chromatogr. A 1410 (2015) 129–139.
[24] X. Zheng, S. Zhu, S. Chang, Y. Cao, J. Dong, J. Li, R. Long, Y. Zhou, Protective effects of chronic resveratrol treatment on vascular inflammatory injury in streptozotocin-induced type 2 diabetic rats: role of NF-kappa B signaling, Eur. J. Pharmacol. (2013).
[25] S.H. Eo, H. Cho, S.J. Kim, Resveratrol inhibits nitric oxide-induced apoptosis via the NF-kappa B pathway in rabbit articular chondrocytes, Biomol. Ther. 21 (2013) 364–370.
[26] D.A. Benitez, M.A. Hermoso, E. Pozo-Guisado, P.M. Fernandez-Salguero, E.A. Castellon, Regulation of cell survival by resveratrol involves inhibition of NF kappa B-regulated gene expression in prostate cancer cells, Prostate 69 (2009) 1045–1054.
[27] C. de Melo Wde, A.N. Lee, J.R. Perussi, M.R. Hamblin, Electroporation enhances antimicrobial photodynamic therapy mediated by the hydrophobic photosensitizer, hypericin, Photodiagnosis Photodyn. Ther. 10 (2013) 647–650.
[28] C.R. Teixeira, M.J. Teixeira, R.B. Gomes, C.S. Santos, B.B. Andrade, I. Raffaele-Netto, J.S. Silva, A. Guglielmotti, J.C. Miranda, A. Barral, C. Brodskyn, M. Barral-Netto, Saliva from *Lutzomyia longipalpis* induces CC chemokine ligand 2/monocyte chemoattractant protein-1 expression and macrophage recruitment, J. Immunol. 175 (2005) 8346–8353.
[29] J.C. Edwards, A.D. Sedgwick, D.A. Willoughby, The formation of a structure with the features of synovial lining by subcutaneous injection of air: an *in vivo* tissue culture system, J. Pathol. 134 (1981) 147–156.
[30] D.P. Dos Santos, I.P.R. Muniz, A.F. Queiroz, I.S. Pereira, M.P.A. Souza, L.J. Lima, L.R.O. Sousa, I.S. Ribeiro, M.P.L. Galantini, L.M. Marques, T.B. Figueiredo, R.A.A. da Silva, Individual variation is the key to the development of a vaccine against *Staphylococcus aureus*: a comparative study between mice lineages, Braz. J. Med. Biol. Res. 51 (2018) e6773.
[31] D. Uesugia, H. Hamada, K. Shimoda, Glycosylation of trans-resveratrol by cultured plant cells under illumination of LEDs, Nat. Prod. Commun. 11 (2016) 199–200.
[32] S. Iida, Y. Ohkubo, Y. Yamamoto, A. Fujisawa, Parabanic acid is the singlet oxygen specific oxidation product of uric acid, J. Clin. Biochem. Nutr. 61 (2017) 169–175.
[33] F. Fischer, G. Graschew, H.J. Sinn, W. Maier-Borst, W.J. Lorenz, P.M. Schlag, A chemical dosimeter for the determination of the photodynamic activity of photosensitizers, Clin. Chim. Acta; Int. J. Clin. Chem. 274 (1998) 89–104.
[34] T. Maisch, J. Baier, B. Franz, M. Maier, M. Landthaler, R.M. Szeimies, W. Baumler, The role of singlet oxygen and oxygen concentration in photodynamic inactivation of bacteria, Proc. Natl. Acad. Sci. U. S. A. 104 (2007) 7223–7228.
[35] S. Al-Omari, A. Ali, Photodynamic activity of pyropheophorbide methyl ester and pyropheophorbide a in dimethylformamide solution, Gen. Physiol. Biophys. 28 (2009) 70–77.
[36] H.N. Jiang, Y. Li, Z.J. Cui, Photodynamic physiology-photonanomanipulations in cellular physiology with protein photosensitizers, Front. Physiol. 8 (2017) 191.
[37] X. Ragas, X. He, M. Agut, M. Roxo-Rosa, A.R. Gonsalves, A.C. Serra, S. Nonell, Singlet oxygen in antimicrobial photodynamic therapy: photosensitizer-dependent production and decay in E. coli, Molecules 18 (2013) 2712–2725.
[38] T.A. Dahl, W.R. Midden, P.E. Hartman, Pure singlet oxygen cytotoxicity for bacteria, Photochem. Photobiol. 46 (1987) 345–352.
[39] A.L. Cogen, V. Nizet, R.L. Gallo, Skin microbiota: a source of disease or defence? Br. J. Dermatol. 158 (2008) 442–455.
[40] T. Kane, K. Carothers, S. Lee, Virulence factor targeting of the bacterial pathogen *Staphylococcus aureus* for vaccine and therapeutics, Curr. Drug Targets (2016).
[41] B.K. Giersing, S.S. Dastgheyb, K. Modjarrad, V. Moorthy, Status of vaccine research and development of vaccines for *Staphylococcus aureus*, Vaccine 34 (2016) 2962–2966.
[42] L.P. Rosa, F.C. Silva, S.A. Nader, G.A. Meira, M.S. Viana, Effectiveness of antimicrobial photodynamic therapy using a 660 nm laser and methyline blue dye for inactivating *Staphylococcus aureus* biofilms in compact and cancellous bones: an *in vitro* study, Photodiagnosis Photodyn. Ther. 12 (2015) 276–281.
[43] K. Morimoto, T. Ozawa, K. Awazu, N. Ito, N. Honda, S. Matsumoto, D. Tsuruta, Photodynamic therapy using systemic administration of 5-aminolevulinic acid and a 410-nm wavelength light-emitting diode for methicillin-resistant *Staphylococcus aureus*-infected ulcers in mice, PLoS One 9 (2014) e105173.
[44] R.T. Kashiwabuchi, Y. Khan, F.R. Carvalho, F. Hirai, M.S. Campos, P.J. McDonnell, Antimicrobial susceptibility of photodynamic therapy (UVA/riboflavin) against *Staphylococcus aureus*, Arq. Bras. Oftalmol. 75 (2012) 423–426.
[45] X.J. Fu, Y. Fang, M. Yao, Antimicrobial photodynamic therapy for methicillin-resistant *Staphylococcus aureus* infection, Biomed Res. Int. 2013 (2013) 159157.
[46] N. Tortik, A. Spaeth, K. Plaetzer, Photodynamic decontamination of foodstuff from *Staphylococcus aureus* based on novel formulations of curcumin, Photochem. Photobiol. Sci. 13 (2014) 1402–1409.
[47] H.J. Park, Y.H. Moon, H.E. Yoon, Y.M. Park, J.H. Yoon, I.S. Bang, Agr function is upregulated by photodynamic therapy for *Staphylococcus aureus* and is related to resistance to photodynamic therapy, Microbiol. Immunol. 57 (2013) 547–552.
[48] R. Al-Mutairi, A. Tovmasyan, I. Batinic-Haberle, L. Benov, Sublethal photodynamic treatment does not lead to development of resistance, Front. Microbiol. 9 (2018) 1699.
[49] N. Kashef, M.R. Hamblin, Can microbial cells develop resistance to oxidative stress in antimicrobial photodynamic inactivation? Drug Resist. Update 31 (2017) 31–42.
[50] M. Grinholc, B. Szramka, K. Olender, A. Graczyk, Bactericidal effect of photodynamic therapy against methicillin-resistant *Staphylococcus aureus* strain with the use of various porphyrin photosensitizers, Acta Biochim. Pol. 54 (2007) 665–670.
[51] C.M. Cassidy, R.F. Donnelly, M.M. Tunney, Effect of sub-lethal challenge with Photodynamic Antimicrobial Chemotherapy (PACT) on the antibiotic susceptibility of clinical bacterial isolates, J. Photochem. Photobiol. B Biol. 99 (2010) 62–66.
[52] S.H. Selman, G.M. Garbo, R.W. Keck, M. Kreimer-Birnbaum, A.R. Morgan, A dose response analysis of purpurin derivatives used as photosensitizers for the photodynamic treatment of transplantable FANFT induced urothelial tumors, J. Urol. 137 (1987) 1255–1257.
[53] V.G. Garcia, M. Longo, E.C. Gualberto Junior, A.F. Bosco, M.J. Nagata, E. Ervolino, L.H. Theodoro, Effect of the concentration of phenothiazine photosensitizers in antimicrobial photodynamic therapy on bone loss and the immune inflammatory response of induced periodontitis in rats, J. Periodont. Res. 49 (2014) 584–594.
[54] J. Hempstead, D.P. Jones, A. Ziouche, G.M. Cramer, I. Rizvi, S. Arnason, T. Hasan, J.P. Celli, Low-cost photodynamic therapy devices for global health settings: characterization of battery-powered LED performance and smartphone imaging in 3D tumor models, Sci. Rep. 5 (2015) 10093.
[55] M. Hayashi, H. Fukuhara, K. Inoue, T. Shuin, Y. Hagiya, M. Nakajima, T. Tanaka, S. Ogura, The effect of iron ion on the specificity of photodynamic therapy with 5-aminolevulinic acid, PLoS One 10 (2015) e0122351.
[56] D.A. Musser, A.R. Oseroff, Characteristics of the immunosuppression induced by cutaneous photodynamic therapy: persistence, antigen specificity and cell type involved, Photochem. Photobiol. 73 (2001) 518–524.
[57] A. Mamalis, E. Koo, J. Jagdeo, Resveratrol prevents reactive oxygen species-induced effects of light-emitting diode-generated blue light in human skin fibroblasts, Dermatol. Surg. 42 (2016) 727–732.
[58] V.H. Panhoca, F.L. Esteban Florez, T.Q. Correa, F.R. Paolillo, C.W. de Souza, V.S. Bagnato, Oral decontamination of orthodontic patients using photodynamic therapy mediated by blue-light irradiation and curcumin associated with sodium dodecyl sulfate, Photomed. Laser Surg. 34 (2016) 411–417.
[59] T. Niu, Y. Tian, Q. Cai, Q. Ren, L. Wei, Red light combined with blue light irradiation regulates proliferation and apoptosis in skin keratinocytes in combination with low concentrations of curcumin, PLoS One 10 (2015) e0138754.
[60] D.P. Leite, F.R. Paolillo, T.N. Parmesano, C.R. Fontana, V.S. Bagnato, Effects of photodynamic therapy with blue light and curcumin as mouth rinse for oral disinfection: a randomized controlled trial, Photomed. Laser Surg. 32 (2014) 627–632.
[61] D. Manoil, A. Filieri, C. Gameiro, N. Lange, J. Schrenzel, J.C. Wataha, S. Bouillaguet, Flow cytometric assessment of *Streptococcus mutans* viability after

exposure to blue light-activated curcumin, Photodiagnosis Photodyn. Ther. 11 (2014) 372–379.
[62] J.B. Ribeiro, A.L. Miranda-Vilela, D. Graziani, M.R. Gomes, A.A. Amorim, R.D. Garcia, J. de Souza Filho, A.C. Tedesco, F.L. Primo, J.R. Moreira, A.V. Lima, R.N. Sampaio, Evaluation of the efficacy of systemic miltefosine associated with photodynamic therapy with liposomal chloroaluminium phthalocyanine in the treatment of cutaneous leishmaniasis caused by *Leishmania (L.) amazonensis* in C57BL/6 mice, Photodiagnosis Photodyn. Ther. 13 (2016) 282–290.
[63] D.B. Duarte, M.R. Vasko, J.C. Fehrenbacher, Models of inflammation: carrageenan air pouch, Curr. Protoc. Pharmacol. 72 (5 6) (2016) 1–9.
[64] J.Y. Wu, R.Y. Zhou, X. Jiang, Q. Wu, H. Zhang, Effects of TNF-alpha, IFN-gamma on the ability of keratinocytes to kill intracellular *Staphylococcus aureus*, Sichuan da xue xue bao. Yi xue ban = J. Sichuan Univ. Med. Sci. Ed. 43 (2012) 382–385.
[65] R. Kapetanovic, M. Parlato, C. Fitting, V. Quesniaux, J.M. Cavaillon, M. Adib-Conquy, Mechanisms of TNF induction by heat-killed *Staphylococcus aureus* differ upon the origin of mononuclear phagocytes, Am. J. Physiol. Cell Physiol. 300 (2011) C850–859.
[66] N.K. Archer, J.M. Harro, M.E. Shirtliff, Clearance of *Staphylococcus aureus* nasal carriage is T cell dependent and mediated through interleukin-17A expression and neutrophil influx, Infect. Immun. 81 (2013) 2070–2075.
[67] D.J. Cua, C.M. Tato, Innate IL-17-producing cells: the sentinels of the immune system, Nat. Rev. Immunol. 10 (2010) 479–489.
[68] J.L. Werner, M.A. Gessner, L.M. Lilly, M.P. Nelson, A.E. Metz, D. Horn, C.W. Dunaway, J. Deshane, D.D. Chaplin, C.T. Weaver, G.D. Brown, C. Steele, Neutrophils produce interleukin 17A (IL-17A) in a dectin-1- and IL-23-dependent manner during invasive fungal infection, Infect. Immun. 79 (2011) 3966–3977.
[69] K. Ley, E. Smith, M.A. Stark, IL-17A-producing neutrophil-regulatory Tn lymphocytes, Immunol. Res. 34 (2006) 229–242.
[70] S. Cypowyj, C. Picard, L. Marodi, J.L. Casanova, A. Puel, Immunity to infection in IL-17-deficient mice and humans, Eur. J. Immunol. 42 (2012) 2246–2254.
[71] L. Lin, A.S. Ibrahim, X. Xu, J.M. Farber, V. Avanesian, B. Baquir, Y. Fu, S.W. French, J.E. Edwards Jr., B. Spellberg, Th1-Th17 cells mediate protective adaptive immunity against *Staphylococcus aureus* and *Candida albicans* infection in mice, PLoS Pathog. 5 (2009) e1000703.
[72] S. Evans, W. Matthews, R. Perry, D. Fraker, J. Norton, H.I. Pass, Effect of photodynamic therapy on tumor necrosis factor production by murine macrophages, J. Natl. Cancer Inst. 82 (1990) 34–39.
[73] E. Szliszka, A. Kawczyk-Krupka, Z.P. Czuba, A. Sieron, W. Krol, Effect of ALA-mediated photodynamic therapy in combination with tumor necrosis factor-related apoptosis-inducing ligand (TRAIL) on bladder cancer cells, Cent. European J. Urol. 64 (2011) 175–179.
[74] P. Ziolkowski, K. Symonowicz, J. Milach, B. Zawirska, T. Szkudlarek, *In vivo* tumor necrosis factor-alpha induction following chlorin e6-photodynamic therapy in Buffalo rats, Neoplasma 44 (1997) 192–196.
[75] D.A. Bellnier, Potentiation of photodynamic therapy in mice with recombinant human tumor necrosis factor-alpha, J. Photochem. Photobiol. B Biol. 8 (1991) 203–210.
[76] Y.Y. Huang, M. Tanaka, D. Vecchio, M. Garcia-Diaz, J. Chang, Y. Morimoto, M.R. Hamblin, Photodynamic therapy induces an immune response against a bacterial pathogen, Expert Rev. Clin. Immunol. 8 (2012) 479–494.
[77] R.W. Steubing, S. Yeturu, A. Tuccillo, C.H. Sun, M.W. Berns, Activation of macrophages by Photofrin II during photodynamic therapy, J. Photochem. Photobiol. B Biol 10 (1991) 133–145.
[78] R. Li, Y. Zhang, M.A. Mohamed, X. Wei, C. Cheng, Macrophages play an essential role in the long effects of low-dose photodynamic therapy on vessel permeability, Int. J. Biochem. Cell Biol. 71 (2016) 55–61.
[79] M.F. Pansa, M.J. Lamberti, I.S. Cogno, S.G. Correa, N.B. Rumie Vittar, V.A. Rivarola, Contribution of resident and recruited macrophages to the photodynamic intervention of colorectal tumor microenvironment, Tumour Biol. 37 (2016) 541–552.
[80] U.N. Das, M. Padma, P.S. Sagar, G. Ramesh, R. Koratkar, Stimulation of free radical generation in human leukocytes by various agents including tumor necrosis factor is a calmodulin dependent process, Biochem. Biophys. Res. Commun. 167 (1990) 1030–1036.
[81] M. Larysz-Brysz, J. Lewin-Kowalik, Z. Czuba, K. Kotulska, E. Olakowska, W. Marcol, A. Liskiewicz, H. Jedrzejowska-Szypulka, Interleukin-1beta increases release of endothelin-1 and tumor necrosis factor as well as reactive oxygen species by peripheral leukocytes during experimental subarachnoid hemorrhage, Curr. Neurovasc. Res. 9 (2012) 159–166.
[82] S.I. Jeong, J.A. Shin, S. Cho, H.W. Kim, J.Y. Lee, J.L. Kang, E.M. Park, Resveratrol attenuates peripheral and brain inflammation and reduces ischemic brain injury in aged female mice, Neurobiol. Aging 44 (2016) 74–84.
[83] Y. Liu, J. Mei, L. Gonzales, G. Yang, N. Dai, P. Wang, P. Zhang, M. Favara, K.C. Malcolm, S. Guttentag, G.S. Worthen, IL-17A and TNF-alpha exert synergistic effects on expression of CXCL5 by alveolar type II cells *in vivo* and *in vitro*, J. Immunol. 186 (2011) 3197–3205.
[84] H.M. Lauridsen, A.S. Pellowe, A. Ramanathan, R. Liu, K. Miller-Jensen, J.M. McNiff, J.S. Pober, A.L. Gonzalez, Tumor necrosis factor-alpha and IL-17A activation induces pericyte-mediated basement membrane remodeling in human neutrophilic dermatoses, Am. J. Pathol. 187 (2017) 1893–1906.
[85] S.S. Iyer, G. Cheng, Role of interleukin 10 transcriptional regulation in inflammation and autoimmune disease, Crit. Rev. Immunol. 32 (2012) 23–63.